Published in final edited form as:
Cytokine. 2013 March ; 61(3): 924–932. doi:10.1016/j.cyto.2012.12.015.

Functional Characterization of Ferret CCL20 and CCR6 and Identification of Chemotactic Inhibitors

Shulin Qin[a], **Cynthia R. Klamar**[a], **Beth A. Fallert Junecko**[a], **Jodi Craigo**[b,c], **Deborah H. Fuller**[d], and **Todd A. Reinhart**[a,*]

[a]Department of Infectious Diseases and Microbiology, Graduate School of Public Health, University of Pittsburgh, 130 DeSoto Street, Pittsburgh, PA 15261

[b]Department of Microbiology and Molecular Genetics, University of Pittsburgh School of Medicine, Pittsburgh, PA 15261

[c]Center for Vaccine Research, University of Pittsburgh, Pittsburgh, PA 15261

[d]Department of Microbiology, University of Washington, Box 357735, Seattle, WA 98195

Abstract

CCL20 is currently the only known chemokine ligand for the receptor CCR6, and is a mucosal chemokine involved in normal and pathological immune responses. Although nucleotide sequence data are available for *ccl20* and *ccr6* sequences from multiple species, the ferret *ccl20* and *ccr6* sequences have not been determined. To increase our understanding of immune function in ferret models of infection and vaccination, we have used RT-PCR to obtain the ferret *ccl20* and *ccr6* cDNA sequences and functionally characterize the encoded proteins. The open reading frames of both genes were highly conserved across species and mostly closely related to canine sequences. For functional analyses, single cell clones expressing ferret CCR6 were generated, a ferret CCL20/mouse IgG_{2a} fusion protein (fCCL20-mIgG_{2a}) was produced, and fCCL20 was chemically synthesized. Cell clones expressing ferret CCR6 responded chemotactically to fCCL20-mIgG2a fusion protein and synthetic ferret CCL20. Chemotaxis inhibition studies identified the polyphenol epigallocatechin-3-gallate and the murine γ-herpesvirus 68 M3 protein as inhibitors of fCCL20. Surface plasmon resonance studies revealed that EGCG bound directly to fCCL20. These results provide molecular characterization of previously unreported ferret immune gene sequences and for the first time identify a broad-spectrum small molecule inhibitor of CCL20 and reveal CCL20 as a target for the herpesviral M3 protein.

Keywords

chemokine; CCL20; CCR6; ferret; EGCG; M3 protein

*Corresponding author: Tel., 412-648-2341; reinhar@pitt.edu; Department of Infectious Diseases and Microbiology, Graduate School of Public Health, University of Pittsburgh, 606 Parran Hall, 130 DeSoto Street, Pittsburgh, PA 15261.

1. Introduction

Chemokines are a family of small cytokines that mediate leukocyte chemotaxis [1]. This family of immunomodulatory proteins has been divided into four major families on the basis of the spacing of the most amino-terminal of four conserved cysteine residues, including the C, CC, CXC, and CX3C families. In addition, they can be grouped into homeostatic and inflammatory chemokines based on the extent to which they contribute to constitutive or induced host responses. Chemokines have additional and diverse functions, including hematopoiesis and lymphoid organ development, T-lymphocyte maturation [2], antimicrobial activities [3, 4], and in some cases protection of cells from apoptosis [5–7]. Chemokines also are involved in multiple aspects of immunological disease processes, including chronic inflammation and infectious diseases [2].

The chemokine CCL20 is involved in normal and pathological immune processes and is the only identified chemokine ligand of chemokine receptor CCR6 [8–10], although β–defensins are also chemotactic via CCR6 signaling [11]. The majority of chemokine cDNA sequences that have been reported are human and murine, along with a small number of other species, but there is limited, albeit growing, information regarding ferret chemokine sequences. Ferrets are being studied for host/pathogen interactions to understand pathology and respiratory diseases, particularly as challenge models to evaluate new vaccines and antivirals against seasonal and pandemic influenza [12–16]. Data on the similarities and differences between components of ferret model systems and human immune responses and disease will provide critical information and resources that could be translated to humans. With these purposes in mind, we have cloned and sequenced ferret *ccl20* and *ccr6* cDNAs directly from ferret tissues, performed phylogenetic comparisons with other species, developed functional chemotactic assays for fCCL20 and fCCR6, and identified epigallocatechin-3-gallate (EGCG) and murine γ-herpesvirus 68 (MHV68) M3 protein as inhibitors of fCCL20. These findings and reagents expand our understanding and repertoire of tools for study of ferret responses to vaccination and infection.

2. Materials and Methods

2.1. Cloning of ferret ccl20 and ccr6 partial cDNAs

Total cellular RNAs were prepared by homogenization of ferret liver and spleen tissues (kindly provided by Dr. Ted Ross) using Trizol (Life Technologies, Rockville, MA, USA) according to the manufacturer's recommendations. Reverse transcription was performed using oligo(dT) primers (Reverse Transcription System, Promega, Madison, WI), and resulting cDNAs were amplified by PCR using gene-specific primers (SQ_fCCL20_F1: 5′-ATG TGC AGT AGC AAG AAT TTG CTC -3′; SQ_fCCL20_R1: 5′-TTA CAT CTT CTT GAC TCT ATG GCT GAG GA-3′ and SQ_fCCR6_F8: 5′-CAG GTC ACA CGA CAG CTA AC-3′; SQ_fCCR6_R2: 5′-TCA CAT GGT GAA GGA CGA-3′) which were designed based on the canine sequences available in the GenBank database (accession numbers AB164385 and XM_541197). The PCR program used was: one cycle for 3min at 94°C; 30 cycles of 30sec at 94°C, 30sec at 56°C, and 2min at 72°C; and a final extension for 10min at 72°C. Amplified products were agarose gel purified and ligated to the pGEM-T cloning vector (Promega). Insert-containing clones were identified and DNA sequenced (Genomics and Proteomics Core Laboratories, University of Pittsburgh). The assigned GenBank accession numbers are JX462946 for *ccl20* and JX462947 for ferret *ccr6*.

2.2. DNA sequence analysis

The Molecular Evolutionary Genetics Analysis version 5 (MEGA5) [17] software package was used for phylogenetic analysis of ferret *ccl20* and *ccr6* partial cDNA and deduced amino acid sequences. This software uses the neighbor joining method to align sequences

and generate phylogenetic trees with the CLUSTAL W algorithm. The *ccl20* and *ccr6* sequences from other species were obtained from the GenBank database. The GenBank accession numbers of these *ccl20* sequences were canine (AB164385), porcine (NM-001024589), bovine (NM_174263), macaque (NM-001032854), human (BC020698), chimpanzee (XM_516133), hamster (AY924377), murine (BC028504) and rat (NM_019233). The GenBank accession numbers of the *ccr6* sequences were canine (XM_541197), bovine (NM-001194961), rabbit (XM_002723866), equine (XM_001489474), macaque (NM-001032935), human (AY242126), chimpanzee (XM_003311584), murine (BC105669) and rat (NM_001013145). Signal peptide cleavage sites, giving rise to the mature amino termini of CCL20, were predicted using the SignalP prediction program (http://www.cbs.dtu.dk/services/SignalP/).

2.3. Chemical synthesis of fCCL20

Synthesis of fCCL20 was performed on an Applied Biosystems 433A synthesizer using HBTU activation with Fmoc/NMP chemistry (University of Pittsburgh Peptide Synthesis Core). Chain elongation was carried out in a stepwise fashion on Novabiochem Fmoc-Met-Wang resin LL (0.27mmole/g) using extended coupling times for all cycles. Amino acid derivatives were from Peptides International and contained the following side-chain protecting groups: Trt for Cys6, Cys32, Asn and Gln; Acm for Cys7 and Cys48; OtBu for Asp and Glu; tBu for Ser; Boc for Lys; and Pbf for Arg. Pseudoproline dipeptides [Fmoc-Ala-Ser(ΨMe,Mepro)-OH; Fmoc-Ile-Thr(ΨMe,Mepro)-OH and Fmoc-Lys(Boc) Thr(ΨMe,Mepro)-OH] from Novabiochem were also incorporated where appropriate to eliminate the occurrence of peptide aggregates during synthesis. Simultaneous cleavage of the peptides from the resin along with removal of side chain protecting groups and conversion of the oxazolidine pseudoprolines to their corresponding amino acid residues was achieved using standard TFA cleavage conditions. This involved treatment of the fully protected peptide resins with Reagent R (TFA:thioanisole:anisole:EDT) (18:1:0.4:0.6 v/v/v) at a concentration of 20ml/gm for 4 hr at room temperature. Filtration of the mixtures through Buchner funnels was followed by precipitation of the peptides in cold diethyl ether and centrifugation. After discarding the supernatants, the resulting pellets were resuspended in cold diethyl ether followed by centrifugation. This procedure was repeated two additional times and the pellets were then dissolved in 0.1%TFA (aqueous) and lyophilized to yield the crude bis-Cys(Acm) protected peptide intermediates.

Purification of the crude peptide intermediates was performed on a Waters Delta Prep 4000 Preparative Chromatography System in order to remove residual TFA and scavengers. Elution from a Phenomenex Synergi 4μ Fusion-RP 80A (250 x 21.20mm) preparative HPLC column was performed using a linear gradient of 5% to 70% acetonitrile in 0.1% TFA over 35min at a flow rate of 25ml/min. Air oxidation to form the disulfide bridge between Cys6 and Cys32 of each peptide was accomplished after dissolution in 0.1M ammonium bicarbonate at a concentration of 0.5mg/ml followed by gentle overnight stirring. Completion of the reaction was confirmed by a negative Ellman test and the oxidized product was purified under the above conditions followed by lyophilization. Treatment of the monobridged bis-Cys(Acm) intermediate peptides with iodine/50%AcOH for 30min simultaneously removed the Acm groups and formed a disulfide bridge between Cys7 and Cys48. After quenching the reaction with sodium thiosulfate, the residual AcOH was removed with a rotary evaporator and the products purified by HPLC and lyophilized. Analytical HPLC performed on a Waters Alliance 2695 Separations Module using Empower data analysis software demonstrated a high degree of homogeneity in the final products. An Applied Biosystems Voyager-DE STR BioSpectrometry workstation was used to determine the products were of the correct molecular mass.

2.4. Construction of plasmids expressing IgG fusion constructs of fCCL20 and fCXCL10

To construct plasmids encoding fCCL20 and fCXCL10 IgG fusion proteins, the ferret CCL20 and CXCL10 ORFs were amplified by PCR with primers TRFcfCCL20F1 (5′-GCC GAA TTC ACC ATG TGC AGT AGC AAG AAT TTG CTC-3′) plus TRFcfCCL20R1 (5′-GCC AGA TCT GCC CAT CTT CTT GAC TCT ATG-3′) and TRFcfCXCL10F1 (5′-GCC GAA TTC ACC ATG AAC CAA AGT GCT GTT CTT-3′) plus TRFcfCXCL10R1 (5′-ACC AGA TCT GCC AGG AGA TGT TTT AGA CCT TTC C-3′) and templates pGEMT.fCCL20.1 and pGEMT.fCXCL10, respectively. The amplified and restriction digested fCCL20 and fCXCL10 PCR products were ligated to parallel digested pFUSE-mIgG2A-Fc1 (Invivogen) between the EcoRI and BglII restriction sites, yielding pFUSE-fCCL20.mIgG2A-Fc1and pFUSE-fCXCL10-mIgG2A-Fc1 plasmids that were then DNA sequence confirmed.

2.5. Generation of single cell clones expressing ferret CCR6

To subclone the ferret *ccr6* ORF into the pcDNA3.1(+) expression plasmid (Invitrogen) the ferret *ccr6* ORF was amplified by PCR with primers SQ_f.CCR6.BamHI_F1 (5′-GCC GGA TCC ACC TAC CAG GAG GCG ATG AAT-3′) and SQ_f.CCR6.NotI_R1 (5′-GCC GCG GCC GCT TAT CAC ATG GTG AAG GAC GAC G-3′) and template pGEMT.fCCR6.1. The amplified and restriction digested fCCR6 PCR product was ligated to parallel digested pcDNA3.1(+) (Invitrogen) between the BamHI and NotI restriction sites, generating pcDNA3.1 (+)-fCCR6.1, which was DNA sequence confirmed.

Transfections were performed as described previously [18, 19]. Briefly, the L1.2 murine pre-B cell line [18–20] was electroporated with pcDNA3.1(+)-fCCR6.1, and stably transfected cells were obtained after two rounds of single cell cloning in the presence of 1mg/ml G418 (Life Technologies). The L1.2 cells expressing ferret CCR6 were identified using chemotaxis toward synthetic ferret CCL20.

2.6. Expression of fCCL20 and fCXCL10 IgG fusion proteins

HEK293T cells were transfected with pFUSE-fCCL20-mIgG2a-Fc1 or pFUSE-fCXCL10-mIgG2a-Fc1 using PolyJet DNA Transfection Reagent (SignaGen) according to the manufacturer's instructions. Briefly, the cells were plated in T25 flasks and grown to 75% confluence. Culture medium (DMEM, 5% FBS, L-glutamine, penicillin and streptomycin) was replaced 30 min prior to transfection. Plasmid DNA was diluted in DMEM medium and PolyJet DNA Transfection Reagent was added. The DNA-PolyJet complexes were incubated for 15 min at room temperature and then added dropwise to the cultured cells. After 20 hr, the supernatants were discarded and 5ml of fresh DMEM containing 2.5% FBS was added. The cultured cells were maintained for an additional 48 hr, at which time the supernatants were harvested and filtered through a 0.22um low-protein binding filter (Millipore) and stored at −80°C.

2.7. Cloning and expression of murine γ-herpesvirus 68 M3 protein

Total cellular RNAs were prepared from lysates (kindly provided by Dr. Ana Mora) of 3T3 cells infected by MHV68, using Trizol (Life Technologies, Rockville, MA) and the RNeasy mini kit (Qiagen) according to the manufacturer's recommendations. Reverse transcription was performed using oligo(dT) primers (Reverse Transcription System, Promega), and resulting cDNAs were amplified by PCR using the gene-specific primers SQ_MHV68.M3.BamHI_F1 (5′-GCC GGA TCC GCC GCC ATG GCC TTC CTA TCC ACA-3′) and SQ_MHV68.M3.NotI_R1 (5′-GCC GCG GCC GC T AA T CAA TGA TCC CCA AAA TAC T-3′) which were designed based on the MHV68.M3 sequence available in the GenBank database (AF127083). The PCR program used was: one cycle for 3min at

94°C; 30 cycles of 30sec at 94°C, 30sec at 56°C, and 2min at 72°C; and a final extension for 10min at 72°C. The amplified and restriction digested MHV68 M3 PCR product was ligated to parallel digested pcDNA3.1(+) plasmid (Invitrogen) between the BamHI and NotI restriction sites, generating pcDNA3.1(+)-MHV68.M3.4, which was DNA sequence confirmed.

HEK293T cells were transfected with pcDNA3.1(+)-MHV68.M3.4 using PolyJet DNA Transfection Reagent (SignaGen) according to the manufacturer's instructions as described above. Culture supernatants were harvested 48 hr after transfection and filtered through a 0.22um low-protein binding filter (Millipore) and stored at −80°C.

2.8. Chemotaxis and chemotaxis inhibition

Chemotaxis was performed using L1.2.fCCR6 cells presented with different concentrations of chemically synthesized ferret CCL20. Chemotaxis of L1.2.fCCR6 cells was also performed toward culture supernatants containing fCCL20-mIgG2a and fCXCL10-mIgG2a fusion proteins. Chemotaxis inhibition was performed with 100nM ferret CCL20 and co-incubation with EGCG (1–100μM; CAS #989-51-5; Sigma) or culture supernatants containing M3 protein. The 96-well ChemoTx chemotaxis system (NeuroProbe Inc., 5μm pore size) was used for all chemotaxis assays as described [18–20]. L1.2.fCCR6 cells (2×10^5) in 20ul RPMI-1640/0.1% BSA were loaded above the membrane. After incubation for 2h at 37°C, 5% CO_2, the cells on top of the membrane were removed with a scraper and the migrated cells in the bottom wells were counted using a hemacytometer.

2.9. Surface plasmon resonance (SPR) analyses of EGCG binding fCCL20

Binding analyses of synthetic fCCL20 to EGCG were performed on a Biacore 3000 instrument (Biacore Life Sciences, GE Healthcare, Piscataway, NJ). Ferret CCL20 was immobilized onto the flow cell of a CM5 chip by standard amine coupling chemistries to covalently bind the proteins to the dextran matrix. A second flow cell was activated and quenched without a ligand to serve as a reference surface to account for any non-specific binding of EGCG to the dextran matrix of the chip. Two-fold serial dilutions of purified EGCG (starting at 0.125μM) in HBS-EP buffer (0.01M HEPES pH 7.4, 0.15M NaCl, 3mM EDTA, 0.005% surfactant P20; GE Healthcare) were flowed over the surfaces at a rate of 80μl/min for 3 min. Dissociation was allowed to occur for 5 min in buffer only. Upon completion of each association and dissociation cycle, surfaces were pulsed with 0.01M NaOH to regenerate the surface. All measurements were double referenced by subtracting out the response to the reference flow cell surface as well as a buffer only injection. Sensogram results as well as steady state affinity determinations were analyzed in BIAevaluation 4.1.1 software (Biacore Life Sciences).

2.10. Statistical analyses

All statistical analyses were performed using the Minitab software package (State College, PA). Paired t-tests were used to compare in vitro EGCG and M3 protein chemotaxis inhibition data. A p-value of <0.05 was considered significant.

3. Results

3.1. Cloning and sequencing of ferret ccl20 and ccr6 cDNAs

Partial cDNAs containing the ORFs of ferret *ccl20* and *ccr6* were generated using RT-PCR with total RNAs from ferret tissues as template. Gene-specific primers were designed based on canine *ccl20* and *ccr6* sequences available in the GenBank database, and the resulting RT-PCR products were subcloned and DNA sequenced. Sequence alignment and pairwise comparisons revealed that the ferret *ccl20* sequences were most closely related to the canine

and porcine counterparts with 88%–90% identity (Fig. 1), whereas the ferret *ccr6* sequences were most closely related to canine and bovine counterparts with 83–86% identity (Fig. 2). Homology with *ccl20* from other species ranged from 71% to 85% (mean of 80%; Figure 1B), and homology with *ccr6* from other species ranged from 72% to 79% (mean of 76%; Figure 2B). Comparison of the deduced amino acid sequences of ferret CCL20 and CCR6 with the canine, porcine, and bovine counterparts revealed between 81% to 85% identity (Fig. 1B and 2B). Homology with CCL20 from other species ranged from 56% to 80% (mean of 65%; Fig. 1B) whereas homology with CCR6 from other species ranged from 69% to 80% (mean of 74%; Fig. 2B). As expected, there were unique amino acid substitutions and/or insertions/deletions in the ferret CCL20 and CCR6 amino acid sequences (Fig. 1A and 2A). The predicted amino-termini of the mature CCL20 proteins just after the signal peptide cleavage site are shown after the small gap in the sequence alignment in Fig. 1A. The Ala-Ser-Asn series is fully conserved at the immediate amino-terminus, yielding a 71 residue mature peptide in all cases except for rat CCL20, which has an additional histidine substitution (Fig. 1A). In Fig. 2A, the deduced amino acid sequences of CCR6 from different species were aligned. Although highly conserved overall, the extracellular amino-terminus was highly divergent and the sequences of extracellular loops (ECLs) 2 and 3 were more highly divergent compared to the sequences in ECL1 (Fig. 2A).

Phylogenetic analyses of the broad set of *ccl20* and *ccr6* ORF nucleotide sequences were performed to evaluate their evolutionary relationships. These analyses indicated that the *ccl20* and *ccr6* sequences from different species clustered into distinct groups (Fig. 3). One cluster included ferret, dog, wild boar, and cow sequences; a second cluster included macaque, human and chimpanzee sequences; and the third cluster included hamster, mouse and rat sequences (Fig. 3A). These phylogenetic relationships were similar for *ccr6* (Fig. 3B). Taken altogether, these sequencing and phylogenetic analyses demonstrated that ferret *ccl20* and *ccr6* sequences were most closely related to canine, and then to porcine and bovine sequences.

3.2. Chemotactic analysis of fCCL20, fCCL20-IgG2a, and fCCR6

The cDNAs and sequence information they contained were used to establish a functional assay for fCCL20 and fCCR6. Cell clones of the L1.2 murine pre-B cell line expressing fCCR6 were generated by transfection and selection with G418 through two rounds of single cell cloning. Since an antibody to fCCR6 does not exist, chemotactic responsiveness to fCCL20 was used to identify individual cell clones with functional fCCR6. As ligands, we used the ORF sequence information to chemically synthesize the mature, signal peptide cleaved form of fCCL20 and also generated an IgG fusion protein by expression in HEK293T cells. Synthetic fCCL20 induced migration of L1.2.fCCR6 cells in the typical bell-shaped, dose-dependent manner, reaching maximum activity at 100nM (Fig. 4A). Migration toward fCCL20 was fCCR6-dependent since the L1.2 parental cells showed negligible migration toward fCCL20 (Fig. 4B). To determine whether fCCL20 fused to the amino-terminus of murine IgG_{2a} (fCCL20-mIgG_{2a}) would also function as a chemotactic ligand for fCCR6, we performed chemotaxis using supernatants from HEK293T cells expressing the fCCL20-mIgG_{2a} fusion protein. The fCCL20-mIgG_{2a} fusion protein induced chemotaxis of L1.2.fCCR6 cells in a dose-dependent manner (Fig. 4B), whereas supernatants from HEK293T cells expressing fCXCL10 fused to mouse IgG_{2a} (fCXCL10-mIgG_{2a}) did not attract L1.2.fCCR6 cells (Fig. 4B). These results reveal that the cDNAs encoding fCCL20 and fCCR6 produce biologically active ligand and receptor, respectively, and that we have established a chemotaxis system that will allow identification and characterization of inhibitors of fCCL20/fCCR6.

3.3. EGCG inhibits and binds to fCCL20

We have previously reported that the green tea polyphenol EGCG can directly inhibit CXCR3-responsive cell migration toward the murine proinflammatory chemokines CXCL9, CXCL10, and CXCL11 [18]. Based on these findings, we determined whether EGCG could inhibit L1.2.fCCR6 cell migration toward fCCL20. Indeed, migration of L1.2.fCCR6 cells toward synthetic fCCL20 was inhibited by EGCG in a dose-dependent manner (Fig. 5A), with more than 90% inhibition by 100μM EGCG. EGCG was not cytotoxic to these cells as incubation for 24 hours yielded greater than 95% viability in 100μM EGCG (not shown). Surface plasmon resonance (SPR) binding analyses in which EGCG was passed over immobilized fCCL20 demonstrated that EGCG dose-dependently binds directly to fCCL20 (Fig. 5B). Steady state analyses of the binding revealed EGCG had an affinity for fCCL20 in the micromolar range ($KD = 2.96\times10^{-6}$; $\eta^2 = 0.664$).

3.4. M3 inhibits fCCL20-mediated chemotaxis

The M3 protein of MHV68 binds multiple murine and human CC and CXC chemokines with high affinity and inhibits chemokine signaling and action [21–24]. It is not known whether the M3 protein can inhibit CCL20. Therefore, we determined whether MHV68 M3 could inhibit L1.2.fCCR6 cell migration toward fCCL20. Indeed, migration of L1.2.fCCR6 cells toward fCCL20 was inhibited by M3 protein in a dose-dependent manner (Fig. 6A), with more than 95% inhibition by co-incubation with culture supernatant from HEK293T cells expressing M3 protein. Migration toward rhesus macaque CCL20 (rhCCL20) was also inhibited by M3 protein in a dose-dependent manner (Fig. 6B). In contrast, migration of cells toward human CXCL12 was not inhibited by M3 (Fig. 6C), consistent with a previous report [24]. These findings are the first to report that CCL20 is also a target of the MHV68 M3 protein.

4. Discussion

We have presented here the previously unreported nucleotide sequences of the ferret *ccl20* and *ccr6* ORFs, the development of a chemotaxis assay for fCCL20 and fCCR6 functional studies, and the identification of EGCG and the MHV68 M3 protein as inhibitors of fCCL20. The amount of information on ferret gene sequences continues to grow [25], in large part because of the use of the ferret model for studies of seasonal and pandemic influenza pathogenesis and vaccination [12–16]. For example, Herfst *et al.* recently reported that influenza A H5N1 virus can be transmitted between ferrets through airborne transmission [26]. Understanding host responses to infection and mechanisms of vaccine-mediated protection requires the availability of genetic and immunologic tools. The limited ferret nucleotide sequence, cDNA clone, protein/peptide, and monoclonal antibody resources contribute to the challenges of the ferret model. Despite information on a number of genes encoding ferret chemokines, chemokine receptors, and cytokines [25], ferret *ccl20* and *ccr6* were not among the reported sequences. Therefore, the ferret CCL20 and CCR6 cDNA and protein resources presented here will be useful for studying the biological functions of ferret chemokines during health, vaccination, and disease.

Understanding the contribution of CCL20 and its receptor CCR6 to host responses is important to modeling the progression of immunologic and infectious diseases, particular in mucosal tissues where viral transmissions and early replication events often occur. CCL20 has both homeostatic and inflammatory chemotactic activities [27], as well as anti-microbial and anti-viral activities [3, 28, 29], which contribute to the host-protective responses at mucosal sites. CCL20 and CCR6 constitute an integral axis of communication between the innate and adaptive immune systems because of the expression of CCR6 on immature DCs [30, 31]. They also are critical components of effector immune responses since CCR6 is

expressed by Th17 cells, Tregs, and memory T cells [11, 27]. The responsiveness of immature DCs to CCL20 via CCR6 suggests that CCL20 could be used in vaccination strategies to draw antigen presenting cells into the local sites of antigen delivery, an idea explored in a number of studies [32, 33] and now possible in ferret models of immunization.

The results we have presented here revealed that the ferret *ccl20* and *ccr6* sequences are most highly related to canine sequences from amongst those available in the GenBank database. In contrast the ferret and murine *ccl20* and *ccr6* sequences were quite disparate (Fig. 1 and 2), with the ferret sequences being more related to their human counterparts than to murine. These relationships underscore the pressures that likely have led to the co-evolution of the paired chemokine and chemokine receptor sequences in different species.

Chemokines are critical molecules involved in host defense function, but they also contribute to pathological inflammatory processes [2], and the development of inhibitors for chemokines or their receptors remains a promising approach for treatment of inflammatory diseases. EGCG is a remarkable molecule with multiple health benefits, minimal toxicity[34–37], and anti-inflammatory functions [38–41]. Although our understanding of EGCG action continues to grow [18, 42–44], the mechanism(s) by which EGCG is anti-inflammatory have not been completely defined. Here we have shown that EGCG inhibits the chemotactic function of fCCL20 in a dose-dependent manner and does so by binding directly to fCCL20. In our previous analyses, EGCG bound and inhibited the murine CXCR3 ligands CXCL9, CXCL10, and CXCL11 at concentrations as low as 10μM [18]. Here, a higher concentration of EGCG (100μM) was needed to inhibit fCCL20. These results suggest that binding to chemokines is a broad anti-inflammatory mechanism of EGCG action and that there are structural aspects to individual chemokines that affect their susceptibilities to EGCG modulation. Further analyses are required to identify the determinants on CCL20 and other chemokines for EGCG binding as well as the basis for differences in levels of inhibition.

Inhibition of inflammation is also a property of particularly larger viruses, including herpesviruses. MHV68 M3 protein binds murine and human chemokines, including CCL2, CCL3, CCL5, CCL19, CCL21, CXCL8 and CXCL13, blocking chemokine signaling and inhibiting chemokine action [21–24]. However, CCL20 had not been examined as a possible target of M3 inhibition. We have shown here that M3 inhibits both fCCL20 and rhCCL20. The CCL20 motif(s) recognized by M3 must be well conserved, since this viral protein from a murine herpesvirus inhibited both ferret and primate forms of CCL20. This inhibition could provide an advantage for the virus by inhibiting the recruitment of immature DCs into the local milieu and thereby reduce the potency and potentially the nature of any downstream antiviral responses.

Overall these results extend the set of resources available for immunologic studies of ferrets, such as antigen-specific monoclonal antibodies, and for further in vitro and in vivo studies of CCL20 function and inhibition in ferrets. They also provide biochemical and immunomodulatory insights into the anti-inflammatory properties of EGCG and MHV68 M3 protein, which serve as lead molecules for developing safe and target-set specific anti-inflammatory compounds for inflammatory and infectious diseases.

Acknowledgments

The authors thank Dr. Ted Ross for provision of access to ferret tissues post-necropsy, Dr. Anna Mora for provision of cell lysate from MHV68 infected cultured cells, Dr. Chengli Sheng and Ms. Stella Berendam for advice on performing and displaying multiple sequence alignments, and Dr. Kazi Islam and Mr. Ray Yurko for synthesis and analysis of ferret CCL20. This work was supported by NIH grant U01 AI074509 (DHF).

Abbreviations used in this article

CCL20	CC chemokine ligand 20
EGCG	epigallocatechin-3-gallate
SPR	surface plasmon resonance

References

1. Zlotnik A, Yoshie O, Nomiyama H. The chemokine and chemokine receptor superfamilies and their molecular evolution. Genome Biol. 2006; 7:243. [PubMed: 17201934]
2. Rossi D, Zlotnik A. The biology of chemokines and their receptors. Annu Rev Immunol. 2000; 18:217–42. [PubMed: 10837058]
3. Yang D, Chen Q, Hoover DM, Staley P, Tucker KD, Lubkowski J, et al. Many chemokines including CCL20/MIP-3alpha display antimicrobial activity. J Leukoc Biol. 2003; 74:448–55. [PubMed: 12949249]
4. Lafferty MK, Sun L, DeMasi L, Lu W, Garzino-Demo A. CCR6 ligands inhibit HIV by inducing APOBEC3G. Blood. 2010; 115:1564–71. [PubMed: 20023216]
5. Kortesidis A, Zannettino A, Isenmann S, Shi S, Lapidot T, Gronthos S. Stromal-derived factor-1 promotes the growth, survival, and development of human bone marrow stromal stem cells. Blood. 2005; 105:3793–801. [PubMed: 15677562]
6. Qin S, Sui Y, Murphey-Corb MA, Reinhart TA. Association between decreased CXCL12 and CCL25 expression and increased apoptosis in lymphoid tissues of cynomolgus macaques during SIV infection. J Med Primatol. 2008; 37(Suppl 2):46–54. [PubMed: 19187430]
7. Youn BS, Yu KY, Oh J, Lee J, Lee TH, Broxmeyer HE. Role of the CC chemokine receptor 9/TECK interaction in apoptosis. Apoptosis. 2002; 7:271–6. [PubMed: 11997671]
8. Schutyser E, Struyf S, Van Damme J. The CC chemokine CCL20 and its receptor CCR6. Cytokine Growth Factor Rev. 2003; 14:409–26. [PubMed: 12948524]
9. Comerford I, Bunting M, Fenix K, Haylock-Jacobs S, Litchfield W, Harata-Lee Y, et al. An immune paradox: how can the same chemokine axis regulate both immune tolerance and activation?: CCR6/CCL20: a chemokine axis balancing immunological tolerance and inflammation in autoimmune disease. Bioessays. 2010; 32:1067–76. [PubMed: 20954179]
10. Ito T, Carson WFt, Cavassani KA, Connett JM, Kunkel SL. CCR6 as a mediator of immunity in the lung and gut. Exp Cell Res. 2011; 317:613–9. [PubMed: 21376174]
11. Yang D, Chertov O, Bykovskaia SN, Chen Q, Buffo MJ, Shogan J, et al. Beta-defensins: linking innate and adaptive immunity through dendritic and T cell CCR6. Science. 1999; 286:525–8. [PubMed: 10521347]
12. Cameron CM, Cameron MJ, Bermejo-Martin JF, Ran L, Xu L, Turner PV, et al. Gene expression analysis of host innate immune responses during Lethal H5N1 infection in ferrets. J Virol. 2008; 82:11308–17. [PubMed: 18684821]
13. Fang Y, Rowe T, Leon AJ, Banner D, Danesh A, Xu L, et al. Molecular characterization of in vivo adjuvant activity in ferrets vaccinated against influenza virus. J Virol. 2010; 84:8369–88. [PubMed: 20534862]
14. Imai H, Shinya K, Takano R, Kiso M, Muramoto Y, Sakabe S, et al. The HA and NS genes of human H5N1 influenza A virus contribute to high virulence in ferrets. PLoS Pathog. 2010; 6:e1001106. [PubMed: 20862325]
15. Kang YM, Song BM, Lee JS, Kim HS, Seo SH. Pandemic H1N1 influenza virus causes a stronger inflammatory response than seasonal H1N1 influenza virus in ferrets. Arch Virol. 2011; 156:759–67. [PubMed: 21234768]
16. Rowe T, Leon AJ, Crevar CJ, Carter DM, Xu L, Ran L, et al. Modeling host responses in ferrets during A/California/07/2009 influenza infection. Virology. 2010; 401:257–65. [PubMed: 20334888]

17. Tamura K, Peterson D, Peterson N, Stecher G, Nei M, Kumar S. MEGA5: molecular evolutionary genetics analysis using maximum likelihood, evolutionary distance, and maximum parsimony methods. Mol Biol Evol. 2011; 28:2731–9. [PubMed: 21546353]

18. Qin S, Alcorn JF, Craigo JK, Tjoeng C, Tarwater PM, Kolls JK, et al. Epigallocatechin-3-gallate reduces airway inflammation in mice through binding to proinflammatory chemokines and inhibiting inflammatory cell recruitment. J Immunol. 2011; 186:3693–700. [PubMed: 21307292]

19. Qin S, Sui Y, Soloff AC, Junecko BA, Kirschner DE, Murphey-Corb MA, et al. Chemokine and cytokine mediated loss of regulatory T cells in lymph nodes during pathogenic simian immunodeficiency virus infection. J Immunol. 2008; 180:5530–6. [PubMed: 18390737]

20. Fox JM, Najarro P, Smith GL, Struyf S, Proost P, Pease JE. Structure/function relationships of CCR8 agonists and antagonists. Amino-terminal extension of CCL1 by a single amino acid generates a partial agonist. J Biol Chem. 2006; 281:36652–61. [PubMed: 17023422]

21. Jensen KK, Chen SC, Hipkin RW, Wiekowski MT, Schwarz MA, Chou CC, et al. Disruption of CCL21-induced chemotaxis in vitro and in vivo by M3, a chemokine-binding protein encoded by murine gammaherpesvirus 68. J Virol. 2003; 77:624–30. [PubMed: 12477865]

22. Martin AP, Canasto-Chibuque C, Shang L, Rollins BJ, Lira SA. The chemokine decoy receptor M3 blocks CC chemokine ligand 2 and CXC chemokine ligand 13 function in vivo. J Immunol. 2006; 177:7296–302. [PubMed: 17082648]

23. Parry CM, Simas JP, Smith VP, Stewart CA, Minson AC, Efstathiou S, et al. A broad spectrum secreted chemokine binding protein encoded by a herpesvirus. J Exp Med. 2000; 191:573–8. [PubMed: 10662803]

24. van Berkel V, Barrett J, Tiffany HL, Fremont DH, Murphy PM, McFadden G, et al. Identification of a gammaherpesvirus selective chemokine binding protein that inhibits chemokine action. J Virol. 2000; 74:6741–7. [PubMed: 10888612]

25. Camp JV, Svensson TL, McBrayer A, Jonsson CB, Liljestrom P, Bruder CE. De-novo transcriptome sequencing of a normalized cDNA pool from influenza infected ferrets. PLoS One. 2012; 7:e37104. [PubMed: 22606336]

26. Herfst S, Schrauwen EJ, Linster M, Chutinimitkul S, de Wit E, Munster VJ, et al. Airborne transmission of influenza A/H5N1 virus between ferrets. Science. 2012; 336:1534–41. [PubMed: 22723413]

27. Williams IR. CCR6 and CCL20: partners in intestinal immunity and lymphorganogenesis. Ann N Y Acad Sci. 2006; 1072:52–61. [PubMed: 17057190]

28. Hoover DM, Boulegue C, Yang D, Oppenheim JJ, Tucker K, Lu W, et al. The structure of human macrophage inflammatory protein-3alpha /CCL20. Linking antimicrobial and CC chemokine receptor-6-binding activities with human beta-defensins. J Biol Chem. 2002; 277:37647–54. [PubMed: 12149255]

29. Ghosh M, Shen Z, Schaefer TM, Fahey JV, Gupta P, Wira CR. CCL20/MIP3alpha is a novel anti-HIV-1 molecule of the human female reproductive tract. Am J Reprod Immunol. 2009; 62:60–71. [PubMed: 19527233]

30. Osterholzer JJ, Ames T, Polak T, Sonstein J, Moore BB, Chensue SW, et al. CCR2 and CCR6, but not endothelial selectins, mediate the accumulation of immature dendritic cells within the lungs of mice in response to particulate antigen. J Immunol. 2005; 175:874–83. [PubMed: 16002685]

31. Yang D, Howard OM, Chen Q, Oppenheim JJ. Cutting edge: immature dendritic cells generated from monocytes in the presence of TGF-beta 1 express functional C-C chemokine receptor 6. J Immunol. 1999; 163:1737–41. [PubMed: 10438902]

32. Guo JH, Fan MW, Sun JH, Jia R. Fusion of antigen to chemokine CCL20 or CXCL13 strategy to enhance DNA vaccine potency. Int Immunopharmacol. 2009; 9:925–30. [PubMed: 19348967]

33. Tarradas J, Alvarez B, Fraile L, Rosell R, Munoz M, Galindo-Cardiel I, et al. Immunomodulatory effect of swine CCL20 chemokine in DNA vaccination against CSFV. Vet Immunol Immunopathol. 2011; 142:243–51. [PubMed: 21684019]

34. Cabrera C, Artacho R, Gimenez R. Beneficial effects of green tea--a review. J Am Coll Nutr. 2006; 25:79–99. [PubMed: 16582024]

35. Clement Y. Can green tea do that? A literature review of the clinical evidence. Prev Med. 2009; 49:83–7. [PubMed: 19465043]

36. Higdon JV, Frei B. Tea catechins and polyphenols: health effects, metabolism, and antioxidant functions. Crit Rev Food Sci Nutr. 2003; 43:89–143. [PubMed: 12587987]

37. Wolfram S. Effects of green tea and EGCG on cardiovascular and metabolic health. J Am Coll Nutr. 2007; 26:373S–88S. [PubMed: 17906191]

38. Abboud PA, Hake PW, Burroughs TJ, Odoms K, O'Connor M, Mangeshkar P, et al. Therapeutic effect of epigallocatechin-3-gallate in a mouse model of colitis. Eur J Pharmacol. 2008; 579:411–7. [PubMed: 18022615]

39. Ahmed S, Pakozdi A, Koch AE. Regulation of interleukin-1beta-induced chemokine production and matrix metalloproteinase 2 activation by epigallocatechin-3-gallate in rheumatoid arthritis synovial fibroblasts. Arthritis Rheum. 2006; 54:2393–401. [PubMed: 16869002]

40. Ahn HY, Xu Y, Davidge ST. Epigallocatechin-3-O-gallate inhibits TNFalpha-induced monocyte chemotactic protein-1 production from vascular endothelial cells. Life Sci. 2008; 82:964–8. [PubMed: 18397796]

41. Takano K, Nakaima K, Nitta M, Shibata F, Nakagawa H. Inhibitory effect of (−)-epigallocatechin 3-gallate, a polyphenol of green tea, on neutrophil chemotaxis in vitro and in vivo. J Agric Food Chem. 2004; 52:4571–6. [PubMed: 15237969]

42. Lin SK, Chang HH, Chen YJ, Wang CC, Galson DL, Hong CY, et al. Epigallocatechin-3-gallate diminishes CCL2 expression in human osteoblastic cells via up-regulation of phosphatidylinositol 3-Kinase/Akt/Raf-1 interaction: a potential therapeutic benefit for arthritis. Arthritis Rheum. 2008; 58:3145–56. [PubMed: 18821707]

43. Shin HY, Kim SH, Jeong HJ, Kim SY, Shin TY, Um JY, et al. Epigallocatechin-3-gallate inhibits secretion of TNF-alpha, IL-6 and IL-8 through the attenuation of ERK and NF-kappaB in HMC-1 cells. Int Arch Allergy Immunol. 2007; 142:335–44. [PubMed: 17135765]

44. Zhu J, Wang O, Ruan L, Hou X, Cui Y, Wang JM, et al. The green tea polyphenol (−)-epigallocatechin-3-gallate inhibits leukocyte activation by bacterial formylpeptide through the receptor FPR. Int Immunopharmacol. 2009; 9:1126–30. [PubMed: 19426837]

Highlights

- Ferret *ccl20* and *ccr6* cDNA sequences were obtained from ferret tissue RNAs.
- Chemically synthesized fCCL20 was chemotactically active through fCCR6.
- Polyphenol EGCG and murine gamma herpesvirus 68 M3 protein both inhibited fCCL20.

A

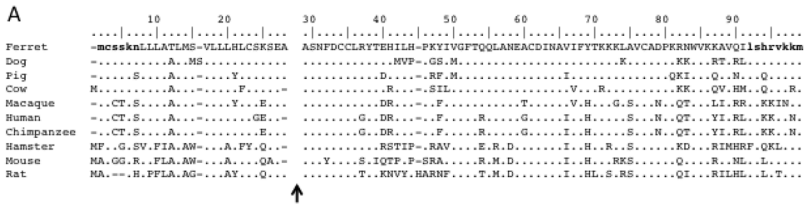

B

Species	Nucleotide sequence identity (%)	Amino acid sequence identity (%)
Dog	90	81
Pig	88	85
Cow	85	80
Macaque	85	73
Human	84	71
Chimpanzee	85	74
Hamster	70	56
Mouse	75	60
Rat	71	56

Fig. 1.

Alignment of the deduced amino acid sequence of fCCL20 with other species. (A) The deduced amino acid sequence of fCCL20 was aligned with the respective sequences from other species using the Clustal W multiple alignment tool in the BioEdit software package. The predicted amino-termini of the mature proteins following signal peptide cleavage have been indicated by the gap and black arrow. Sequences specified by the primers used to obtain the fCCL20 cDNA are indicate by the bold and lower case stretches of deduced amino acids. (B) The relatedness of the ferret *ccl20* nucleotide and amino acid sequences to the *ccl20* sequences available for other species is shown.

A

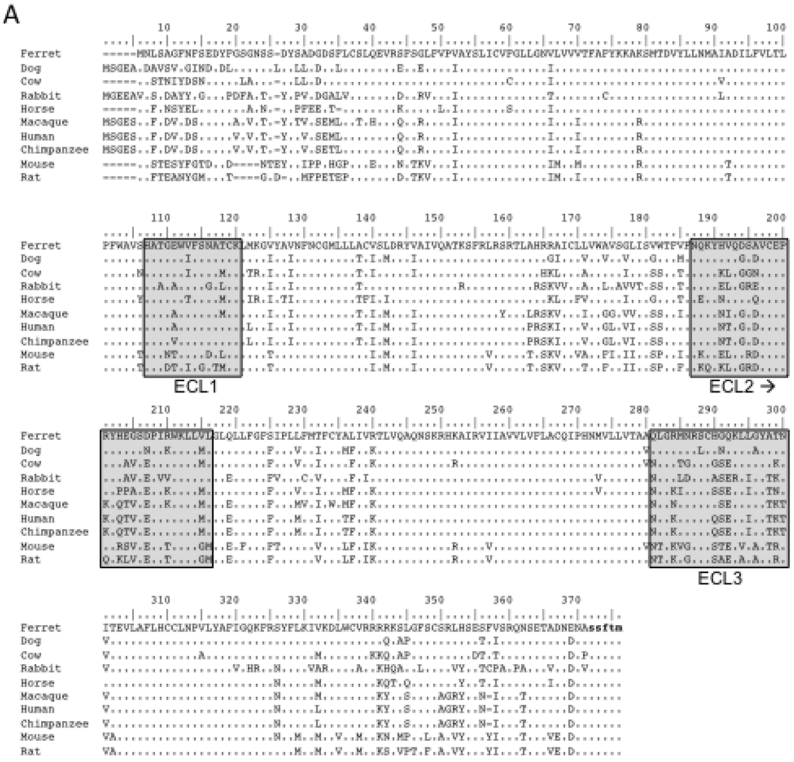

B

Species	Nucleotide sequence identity (%)	Amino acid sequence identity (%)
Dog	86	83
Cow	83	81
Rabbit	79	71
Horse	79	80
Macaque	76	75
Human	76	77
Chimpanzee	76	77
Mouse	72	69
Rat	73	71

Fig. 2.

Alignment of the deduced amino acid sequence of fCCR6 with other species. (A) The deduced amino acid sequence of fCCR6 was aligned with respective sequences from other species. The predicted three extracellular loops (ECLs) are noted by the light grey boxes. Sequences specified by the primers used to obtain the fCCR6 cDNA are indicate by the bold and lower case stretches of deduced amino acids. The forward primer hybridized to sequences upstream of the initial ATG sequence and so is not evident here. (B) The relatedness of the ferret *ccr6* nucleotide and amino acid sequences to the *ccr6* sequences available for other species is shown.

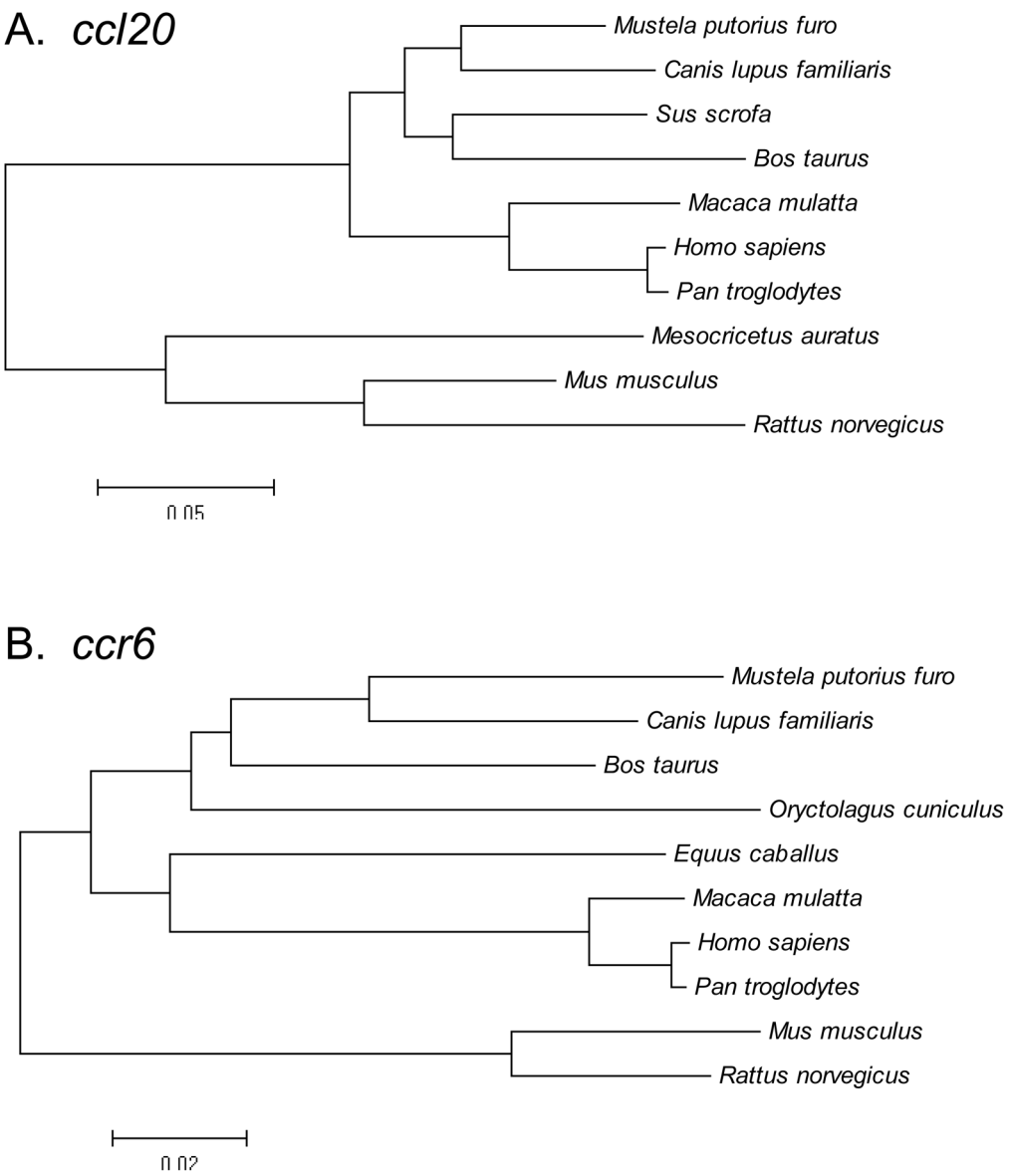

Fig. 3.

Phylogenetic relationships among *ccl20* and *ccr6* cDNA (ORF) sequences from different species. Phylogenetic trees were constructed by the neighbor-joining method, using the MEGA software package following alignment of the (A) *ccl20* and (B) *ccr6* nucleotide sequences.

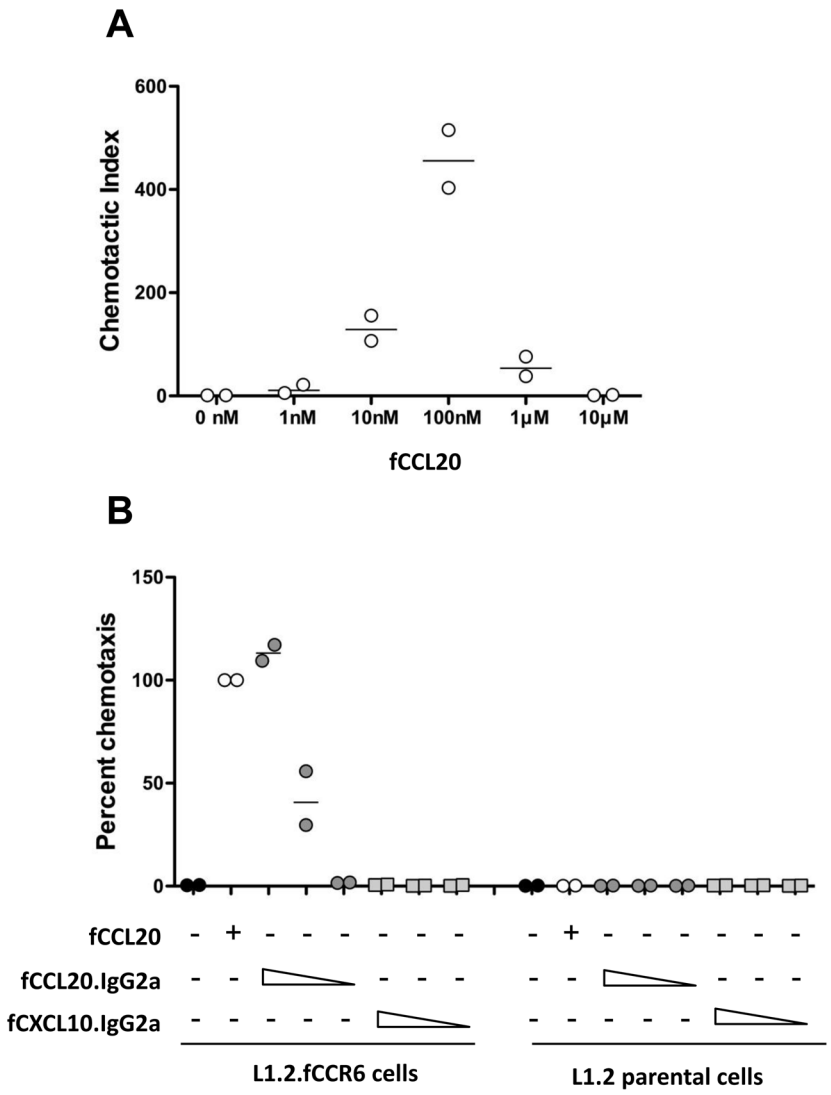

Fig. 4.

Chemotaxis of L1.2.fCCR6 cells toward fCCL20. (A) Chemotaxis of L1.2.fCCR6 cells was performed toward the indicated concentration of synthetic fCCL20. The data are presented as the chemotactic index relative to migration toward no chemokine and are combined from two independent experiments, each performed in triplicate. (B) Chemotaxis of L1.2.fCCR6 cells and L1.2 parental cells was performed toward synthetic fCCL20 (100nM), or toward supernatants from HEK293T cells transiently expressing fCCL20-mIgG_{2a} or fCXCL10-mIgG_{2a} fusion proteins. The supernatants were used neat or at 1:10 or 1:100 dilutions, indicated by the concentration gradient wedges. The data are presented as the percent chemotaxis relative to the synthetic fCCL20 control, and are combined from two independent experiments both performed in triplicate.

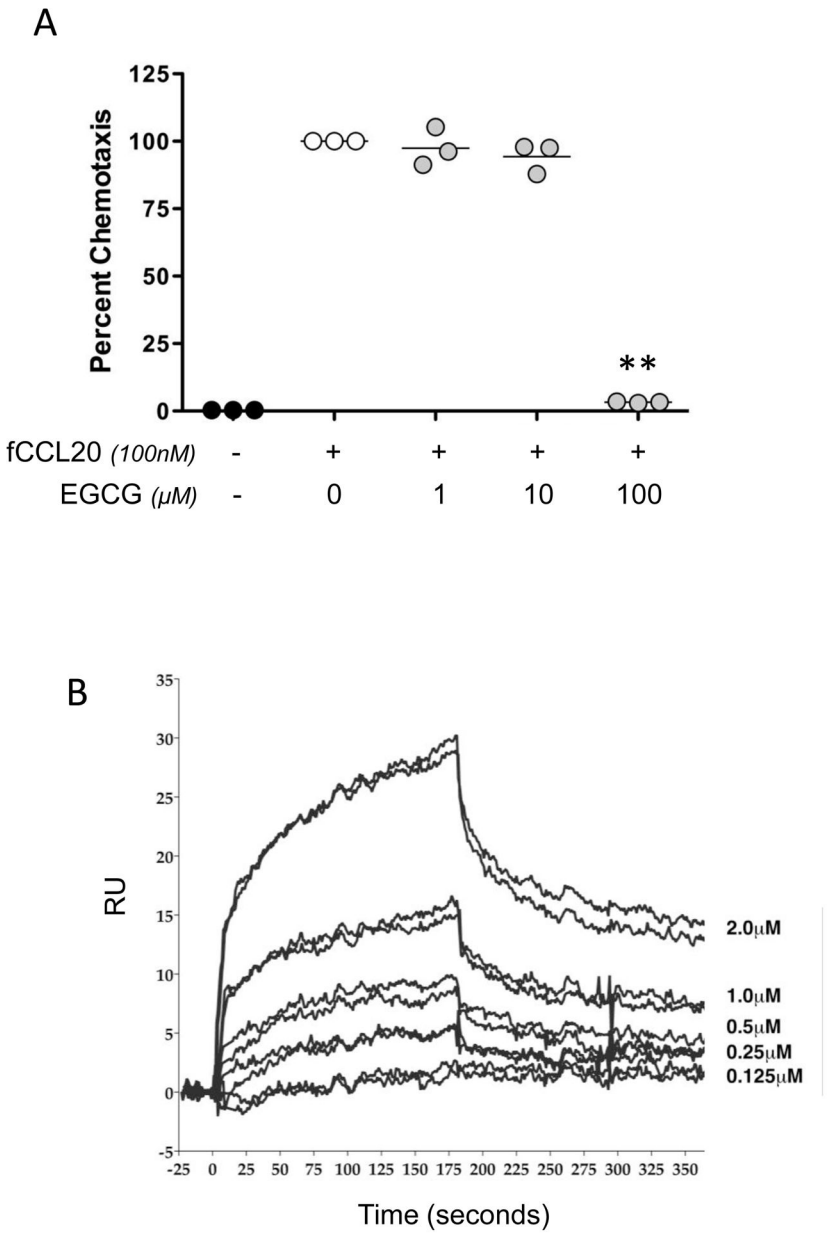

Fig. 5.

EGCG inhibits ferret CCL20. (A) Chemotaxis was performed toward synthetic fCCL20 (100nM) with or without co-incubation of EGCG (1, 10 or 100μM) on the bottom side of the membrane separating L1.2.fCCR6 cells from fCCL20. The data are presented as the percent of control chemotaxis (fCCL20 without co-incubation with EGCG), and were obtained from three independent experiments, each performed in triplicate. The lines in each grouping of data points represents the mean value. Paired *t*-test analyses were performed in comparison to the controls without EGCG and a *P*-value of <0.01 were observed with 100μM EGCG. (B) EGCG binding to fCCL20 was examined using SPR. Sensogram plots provide an indication of binding, response units (RU), over time where association is visualized as an increasing response, during which EGCG was owed over fCCL20. Dissociation is visualized as a decreasing response, during which the solution of EGCG flowing over the chip was replaced with buffer only. Two repeated dose-response curves of

EGCG binding are shown for the indicated two-fold dilutions of EGCG that were injected over immobilized fCCL20.

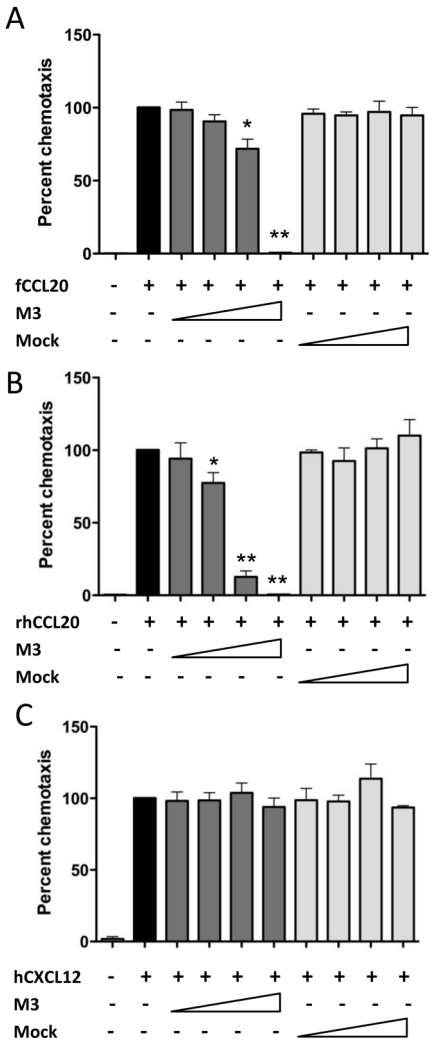

Fig. 6.

M3 protein inhibits CCR6-mediated chemotaxis. (A) Chemotaxis was performed against synthetic fCCL20 (100nM) with or without co-incubation of supernatant from HEK293T cells transiently expressing MHV68 M3 protein (neat, 1:10,1:100 or 1:1000 dilutions) on the bottom side of the membrane separating L1.2.fCCR6 cells from fCCL20. The data are presented as the percent of control chemotaxis observed with fCCL20 alone and are combined from three independent experiments each performed in triplicate. (B) Chemotaxis inhibition was performed as in (A) but with synthetic rhesus macaque CCL20 as the ligand and macaque CCR6-expressing L1.2 cells as the responder cells. (C) Chemotaxis was performed as in (A) but with CXCL12 (1nM) as the ligand and parental L1.2 cells as the responder cells. For all experiments, paired *t*-test analyses were performed to compare migration in the presence of M3 protein to migration in the absence of M3 protein. *P*-values of <0.05 (*) and <0.01(**) were observed with the lower dilutions of M3-containing supernatants.